Theor Chem Acc (2007) 118:75–80
DOI 10.1007/s00214-006-0242-x

REGULAR ARTICLE

Protonated acetylene revisited

Brian T Psciuk · **Victor A. Benderskii** ·
H. Bernhard Schlegel

Received: 6 November 2006 / Accepted: 16 November 2006 / Published online: 20 January 2007

Abstract The potential energy surface for protonated acetylene has been re-examined with large basis sets and highly correlated methods. The energy difference of 3.6–3.8 kcal/mol between the classical structure and non-classical (bridged) structure computed with CCSD (T)/cc-pVQZ, CCSD(T)/6-311+G(3df,2pd), BD(T)/cc-pVQZ, BD(T)/6-311+G(3df,2pd) and CBS-APNO methods is in very good agreement with the best previous calculations, 3.7–4.0 kcal/mol. In contrast, BLYP, B3LYP, PW91, PBE and TPSS density functional methods do rather poorly, yielding −0.52. 0.29, 1.81, 2.16 and 0.62 kcal/mol, respectively, with the 6-311+G(3df,2pd) basis. MP2 calculations predict the classical structure to be a transition state; however, frequency calculations at the CCSD/6-311+G(3df,2pd) level of theory show that the classical structure is a local minimum. CCSD(T), BD(T) and CBS-APNO energy calculations along the MP2/6-311+G(3df,2pd) reaction path indicate that the classical structure is a shallow local minimum separated from the non-classical structure by a very small barrier of 0.11–0.13 kcal/mol. Because the barrier for proton exchange between the non-classical isomers via the classical structure is broad and nearly flat at the top, the tunneling splitting should be reduced, possibly accounting for the 15% difference between the calculated and experimental barrier heights.

Contribution to the Fernando Bernardi Memorial Issue.

B. T. Psciuk · H. B. Schlegel (✉)
Department of Chemistry, Wayne State University,
Detroit, Michigan 48202, USA
e-mail: hbs@chem.wayne.edu

V. A. Benderskii
Institute of Problems of Chemical Physics, RAS,
142432, Moscow Region, Chernogolovka, Russia

1 Introduction

For a seemingly simple molecule, protonated acetylene (vinyl cation) has attracted more than its share of interest and controversy. The structure of carbocations has long been a subject of debate in the physical organic community [1]. Protonated acetylene is one of the simplest carbocations for which classical and non-classical structures can be drawn. This prompted a number of early computational studies [2–6]. While Hartree–Fock calculations favored the classical structure, the addition of electron correlation by perturbation theory or configuration interaction yielded the non-classical ion as the more stable structure. At the other end of the scale, the astrophysical community has become interested in protonated acetylene in connection with the hydrocarbon chemistry of circumstellar and interstellar media (for a overview, see Ref. [7]). This stimulated a number of experimental investigations, and these in turn lead to more detailed theoretical studies in recent years. Although it was detected in the 1930s by mass spectroscopy, protonated acetylene was first observed in IR spectroscopy by Oka and co-workers in 1985 [8]. Coulomb explosion experiments showed that the ion adopted a non-classical structure [9,10]. Further work on the IR spectrum also provided evidence for the non-classical isomer [11,12]. The results of millimeter-wave spectroscopy agreed that protonated acetylene has a non-classical geometry [13–15]. A photoionization study of vinyl radical supplied additional support for the non-classical structure [16]. The energy difference between the classical and non-classical structures is relatively small, leading to tunneling splittings in the rotational and IR spectra of $C_2H_3^+$ [11,14,17]. These splittings imply barrier heights of 1,400–1,600 cm^{-1}.

The experimental probes of the structure and energetics of protonated acetylene prompted quite a number of theoretical studies since the early 1980s. The energy difference between the classical and non-classical structures has been calculated with almost every correlated level for theory—MP2, MP2-R12 [18], MP4 [19], CI [20], CCSD(T) [21,22], MRCI [21,22], ACPF [22], MR-CEPA [23], G1 [24], G2 [25], etc. The basis sets are typically at least triple-zeta quality with multiple polarization functions but often are much larger. Second order Møller–Plesset perturbation theory tends to overestimate the energy difference [18]. MP4 [19], CCSD(T) [21,22] and MRCI [22] calculations are significantly better, predicting energy differences in the range 3.0–4.6 kcal/mol. Lindh et al. [22] have probably carried out the most extensive calculations and find 3.7–4.0 kcal/mol for the classical/non-classical electronic energy difference without zero point energy. By combining their various calculations, their best estimate of the difference is 4.2±0.7 kcal/mol [22]. Vibrational frequency calculations by SCF [26], MP2 [27] and CISD [20] methods with small basis sets predict both the non-classical and classical structures to be local minima, but larger basis MP2 frequency calculations predict the classical structure to be a transition state [22]. For a floppy molecule such as $C_2H_3{}^+$, the rovibrational states are readily classified by non-rigid group theory [28]. The tunneling splittings have been calculated with a number of model Hamiltonians [11,14,15,17,29–31] and are consistent with barriers of 1,400–1,600 cm^{-1} (4–4.5 kcal/mol). The dynamical behavior of $C_2H_3{}^+$ has been simulated using the Car-Parrinello method [32–34]. In this approach, the electron density is propagated by density functional theory using an extended Lagrangian while the nuclear dynamics are treated by classical mechanics or path integral methods. These calculations have shown quantum corrections to be important and have demonstrated that proton exchange occurs by tunneling and thermal activation [33,34].

In the present paper, we have re-examined proton exchange in $C_2H_3{}^+$ in preparation for constructing an analytical function of the potential energy surface. Specifically, we have calculated the reaction path between the classical and non-classical structures, and computed energies along this path at a number of different levels of theory, including CCSD(T), BD(T) and CBS-APNO.

2 Methods

Calculations were performed using the Gaussian suite of programs [35]. Optimized geometries and harmonic vibrational frequencies were calculated with the 6-311+G(d,p) and 6-311+G(3df,2pd) basis sets [36,37] at the MP2 and CCSD levels of theory. Energy differences between the optimized structures were calculated at the MP2, MP4, CCSD, CCSD(T) [38], BD [39] and BD(T) [39] levels of theory with the cc-pVQZ [40] and 6-311+G(3df,2pd) [36,37] basis sets, and with the G2 [41], G3 [42] and CBS-APNO [43] methods. Energy differences were also calculated using BLYP [44,45], B3LYP [46], PW91 [47], PBE [48] and TPSS [49] density functional methods with the 6-311+G(3df,2pd) [36,37] basis set. The intrinsic reaction coordinate (IRC—steepest descent reaction path in mass-weighted Cartesian coordinates) was calculated at the MP2/6-311+G(3df,2pd) level of theory [50]. Single point energy calculations were carried out at points along this path with various levels of theory.

3 Results and discussion

The optimized geometries at various levels of theory are illustrated in Fig. 1. Increasing the basis set from 6-311+G(d,p) to 6-311+G(3df,2pd) shortened the CC and bridging CH bonds by 0.007–0.008 Å, and the non-bridging CH bonds by 0.003–0.005 Å while the angles change by less than 0.2°. Lindh et al. [22] observed similar changes as they increased the basis set. Our results at the MP2/6-311+G(3df,2pd) level agree with MP2/TZ2Pf calculations of Lindh et al. to within a few thousandths of an Ångstrom and fractions of a degree. Improving the level of theory from MP2 to CCSD increased the CC bond by 0.007–0.008 Å and the bridging CH bond by 0.002–0.003 Å; the other CH bonds and angles change very little. These small systematic changes have almost no effect on the energy differences.

The energy differences at various levels of theory are summarized in Table 1. Older work based on Hartree–Fock calculations found the classical structure to be the lowest energy, but all calculations at MP2 and higher levels of electron correlation agree that the non-classical structure is more stable. Energy differences calculated with the cc-pVQZ basis set ([5s,4p,3d,2f,1g/4s,3p,2d,1f], Ref. [40]) and 6-311+G(3df,2pd) [36,37] basis set give results that agree with each other to within 0.1 kcal/mol for a given level of theory. This suggests that the present calculations may be near the basis set limit. Both the MP2 and MP4 calculations overestimate the energy difference, while CCSD underestimates the energy difference. Because the differences in geometry are so small, going from MP2 optimized geometries to CCSD changes the CCSD total energy by less than 0.05 kcal/mol. The triples corrections for the CCSD and BD calculations are quite important, increasing the classical/

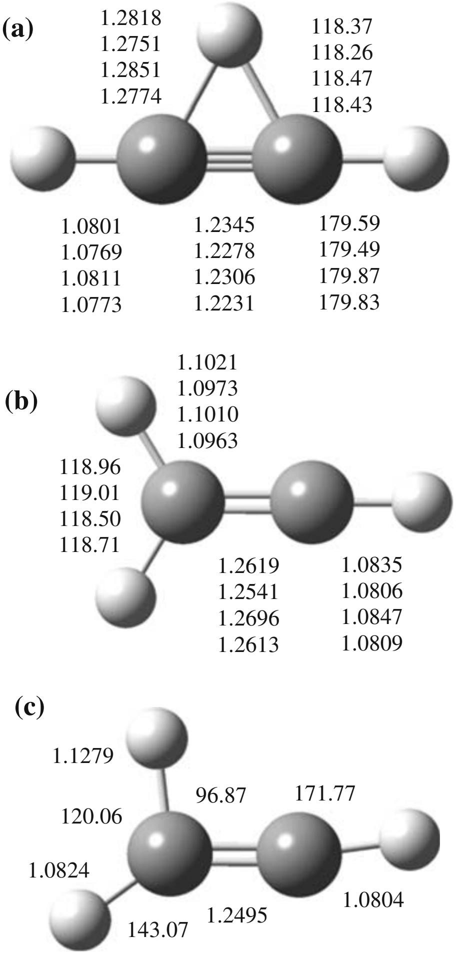

Fig. 1 Optimized geometries of **a** non-classical $C_2H_3{}^+$, **b** classical $C_2H_3{}^+$ and **c** the transition state between the classical and non-classical ions. For **a** and **b**, the values listed from top to bottom are MP2/6-311+G(d,p), MP2/6-311+G(3df,2pd), CCSD/6-311+G(d,p) and CCSD/6-311+G(3df,2pd); for **c** only the CCSD/6-311+G(3df,2pd) values are shown

non-classical energy differences by 0.6–0.9 kcal/mol. In the BD method, the orbitals are optimized to eliminate the T_1 amplitudes in the coupled cluster expansion [39], whereas the CC calculations use the Hartree–Fock orbitals in the reference determinant. The good agreement between the CCSD(T) and BD(T) calculations suggests that the effect of optimizing the orbitals in MCSCF calculations is probably small. The G2 compound method agrees well with the CCSD(T) calculation (as would be expected from the additivity assumptions used in this method [41,42]). The CBS-APNO method extrapolates the MP2 energy to the complete basis set limit and adds corrections from QCISD(T) calculations to account for higher order effects. The present CCSD(T), BD(T) and CBS-APNO calculations agree to within 0.1 kcal/mol with the CCSD(T) calculations of Lindh et al. [22].

Table 1 Energy differences for classical and non-classical protonated acetylene

Theory	ΔE	$E^\ddagger$
MP2	8.69[a], 8.76[b]	
MP4	5.38[a], 5.43[b]	
CCSD	2.78[a], 2.87[b]	0.44[a], 0.42[f], 0.42[g]
CCSD(T)	3.66[a], 3.74[b]	0.07[a], 0.05[f], 0.11[g]
BD	3.06[a], 3.16[b]	0.40[a], 0.37[f], 0.48[g]
BD(T)	3.63[a], 3.71[b]	0.08[a], 0.06[f], 0.13[g]
G2	3.60	
G3	2.92	
CBS-APNO	3.84	0.11[f]
MRCI	4.15[c]	0.66[h]
CEPA	3.61[c]	0.39[h]
CCSD(T)	3.68[d]	
MRCI+Q	4.02[e]	
ACPF	3.93[e]	

In kcal/mol without zero point energy, ΔE = classical – non-classical, $E^\ddagger$ = transition state – classical

[a] cc-pVQZ basis set with the CCSD/6-311+G(3pf,2pd) optimized geometry

[b] 6-311+G(3df,2pd) basis set with the CCSD/6-311+G(3pf,2pd) optimized geometry

[c] [5s 4p 2d 1f/ 3s 2p] ANO basis set with CASSCF/DZP optimized geometry, Ref. [23]

[d] [5s 4p 3d 2f 1g / 4s 3p 2d] ANO basis set with CPF/TZ2P optimized geometry, Ref. [22]

[e] [6s 5p 3d 2f / 4s 3p 2d] ANO basis set with CPF/TZ2P optimized geometry, Ref. [22]

[f] using the CCSD/6-311+G(3pf,2pd) optimized geometries of the transition state and the classical ion

[g] maximum along the MP2/6-311+G(3pf,2pd) reaction path

[h] maximum along the CPF/TZ2P reaction path

Density functional theory (DFT) calculations have been used in Car–Parrinello simulations of the dynamics of protonated acetylene [32–34]. The DFT electronic energy differences (without zero point energy) between the optimized classical and non-classical structures of $C_2H_3{}^+$ are −0.52. 0.29, 1.81, 2.16 and 0.62 kcal/mol with the BLYP, B3LYP, PW91, PBE and TPSS functionals, respectively, using the 6-311+G(3df,2pd) basis set. Similar problems have been noted for propyne—allene isomerization, and for larger hydrocarbon isomer energies (see [51,52] and references therein). Since these popular functionals perform rather poorly on the energy difference, considerable caution is necessary in choosing an appropriate exchange–correlation functional for Car–Parrinello simulations of the dynamics.

The calculated harmonic vibrational frequencies at the stationary points are collected in Table 2. The present MP2 results are in good agreement with the previous MP2/TZ2Pf calculations [22]. With both basis sets, the present MP2 calculations show the classical structure is a transition state with a small imaginary frequency ($72\,i$-$195i$ cm^{-1}). However, the CCSD/6-311+G(d,p) and

Table 2 Harmonic vibrational frequencies and infrared intensities

Symmetry	MP2 6-311+G(d,p)	MP2 6-311+G(3df,2pd)	CCSD 6-311+G(d,p)	CCSD 6-311+G(3df,2pd)	IR Intensity
Non − classical $C_2H_3^+$					
b_2	662.7	706.4	521.8	591.3	25.4
a_2	585.9	604.7	581.1	621.2	0.0
b_1	778.6	764.5	778.8	771.4	106.8
a_1	927.7	916.0	933.8	925.6	46.0
b_2	1312.0	1327.3	1261.0	1280.3	5.0
a_1	1916.9	1926.1	1956.5	1971.4	7.5
a_1	2410.1	2399.8	2394.8	2393.3	80.0
b_2	3311.1	3292.9	3297.1	3282.2	384.5
a_1	3411.4	3393.2	3403.4	3388.9	0.0
Classical $C_2H_3^+$					
b_2	72.4i	194.8i	284.9	240.5	33.9
b_1	685.7	681.9	633.2	632.8	44.2
b_1	823.8	811.3	851.2	851.8	100.6
b_2	1108.2	1095.8	1101.6	1092.0	1.0
a_1	1174.2	1167.5	1205.8	1205.7	77.7
a_1	1754.6	1770.6	1726.1	1745.2	61.7
a_1	3032.4	3033.1	3045.3	3039.9	266.2
b_2	3109.7	3110.2	3119.6	3114.5	189.8
a_1	3337.8	3315.9	3316.6	3303.4	118.8
Classical → non-classical transition-state					
a'				320.6i	48.0
a''				647.3	24.2
a''				805.8	114.5
a'				1036.6	4.4
a'				1167.2	55.7
a'				1822.8	44.8
a'				2833.9	211.2
a'				3229.6	307.0
a'				3320.7	47.3

Frequencies in cm^{-1}, intensities in km/mol at the CCSD/6-311+G(3df,2pd) level of theory

CCSD/6-311+G(3df,2pd) frequency calculations find that the classical structure is a local minimum, with a small positive frequency corresponding to the proton exchange vibrational mode (285 and 240 cm^{-1}, respectively). The fact that earlier calculations found no imaginary frequencies for the classical structure at the SCF [26], MP2 [27] and CISD [20] level is probably an artifact of the small basis sets used in these calculations. However, the large basis set MRCI and CEPA calculations of Lindh et al. [23] do find the classical structure to be a minimum, and find a barrier of 0.4–0.7 kcal/mol for the rearrangement. Pople found a similar transition structure and low barrier at the MP2/6–31G(d) level of theory, but this barrier disappeared at higher levels of theory [19].

To probe the nature of the potential energy surface, we calculated the intrinsic reaction coordinate at the MP2/6-311+G(3df,2pd) level of theory, and obtained the energy at various levels of theory along this path. Like the IRCMAX method [53], this approach assumes that the energy profile perpendicular to the path is less sensitive to the level of theory than the energy profile along the path. The results are shown in Fig. 2. At the MP2 level, the barrier is broad and too high. The MP4 level reduces the barrier significantly, producing a relatively flat profile near the classical structure. The CCSD method underestimates the energy difference and shows a distinct minimum at the classical structure, in agreement with frequency calculations. The minimum still exists at the CCSD(T) level, but is more shallow. The BD and BD(T) calculations parallel the CCSD and CCSD(T) results, respectively. Calculations with the CBS-APNO method yield an energy profile nearly identical to CCSD(T) and BD(T). Thus, our highest levels of theory agree in predicting that the classical structure is a shallow minimum on the potential energy surface. The energy barrier for the classical to non-classical rearrangement is only 0.11–0.13 kcal/mol, most likely too small to support a bound vibrational level for the classical structure. Nevertheless, the shape of the barrier should have an affect on the tunneling splitting. The broad and flat nature of the energy profile should reduce the tunneling splitting from what might be estimated from the barrier height alone. This may contribute to the difference between the barrier height deduced from

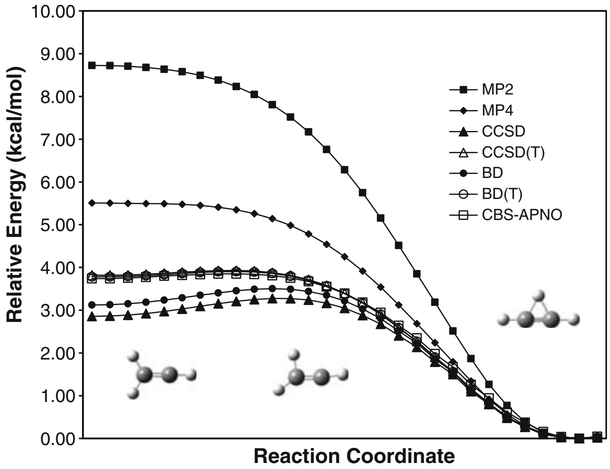

Fig. 2 Energy profiles along the MP2/6-311+G(3df,2pd) intrinsic reaction coordinate at the MP2, MP4, CCSD, CCSD(T), BD and BD(T) levels of theory with the 6-311+G(3df,2pd) basis and CBS-APNO level of theory

experiment and obtained from the highest level calculations.

The CCSD energy profile along the IRC was used as a starting point for optimizing the transition state. The CCSD/6-311+G(3df,2pd) optimized geometry is shown in Fig. 1c, and vibrational frequency calculations at the same level confirm this structure is a transition state (see Table 2). The energy and geometry are nearly identical to maximum along reaction path, thus validating the approach used for Figure 2. The present estimate of the barrier along the reaction path, 0.11–0.13 kcal/mol, is somewhat smaller than the MRCI and CEPA calculations of Lindh et al. [23] (0.7 and 0.4 kcal/mol, respectively). Subsequent electronic structure investigations have not considered the flatness of the $C_2H_3^+$ potential energy surface around the classical ion, and have not looked for a transition state between the classical and non-classical ions. Future dynamics studies will need to take these features of the potential energy surface into account.

4 Conclusions

The potential energy surface for protonated acetylene has been re-examined with large basis sets and highly correlated methods. The computed energy difference between the classical and non-classical structures is in very good agreement with the best previous calculations [22]. However, unlike the most recent calculations, the classical structure is found to be a local minimum, separated from the non-classical structure by a very small barrier. Contrary to past assumptions, the barrier for proton exchange is quite broad with a nearly flat top. This should have a significant effect on the tunneling splitting, and could account for the difference between the calculated and experimental barrier heights.

Acknowledgements This work was supported by a grant from the National Science Foundation (CHE0512144). We thank Dr. Jason L. Sonnenberg for helpful discussions.

References

1. Brown HC, Schleyer PvR (1977) The nonclassical ion problem. Plenum Press, New York
2. Hariharan PC, Lathan WA, Pople JA (1972) Chem Phys Lett 14:385
3. Zurawski B, Ahlrichs R, Kutzelnigg W (1973) Chem Phys Lett 21:309
4. Weber J, Yoshimine M, McLean AD (1976) J Chem Phys 64:4159
5. Lischka H, Koehler HJ (1978) J Am Chem Soc 100:5297
6. Raghavachari K, Whiteside RA, Pople JA, Schleyer PV (1981) J Am Chem Soc 103:5649
7. Greenberg JM, Pirronello V (1991) Chemistry in space. Kluwer Academic Publishers, Dordrecht
8. Crofton MW, Oka T (1985) Proceedings of the fortieth symposium on molecular spectroscopy, Ohio State University
9. Kanter EP, Vager Z, Both G, Zajfman D (1986) J Chem Phys 85:7487
10. Vager Z, Zajfman D, Graber T, Kanter EP (1993) Phys Rev Lett 71:4319
11. Crofton MW, Jagod MF, Rehfuss BD, Oka T (1989) J Chem Phys 91:5139
12. Gabrys CM, Uy D, Jagod MF, Oka T, Amano T (1995) J Phys Chem 99:15611
13. Bogey M, Cordonnier M, Demuynck C, Destombes JL (1992) Astrophys. J 399:L103
14. Bogey M, Bolvin H, Cordonnier M, Demuynck C, Escribano R, Gomez PC (1994) Can J Phys 72:967
15. Demuynck C (1994) J Mol Spectrosc 168:215
16. Berkowitz J, Mayhew CA, Ruscic B (1988) J Chem Phys 88:7396
17. Cordonnier M, Coudert LH (1996) J Mol Spectrosc 178:59
18. Klopper W, Kutzelnigg W (1990) J Phys Chem 94:5625
19. Pople JA (1987) Chem Phys Lett 137:10
20. Lee TJ, Schaefer HF (1986) J Chem Phys 85:3437
21. Liang C, Hamilton TP, Schaefer HF (1990) J Chem Phys 92:3653
22. Lindh R, Rice JE, Lee TJ (1991) J Chem Phys 94:8008
23. Lindh R, Roos BO, Kraemer WP (1987) Chem Phys Lett 139:407
24. Curtiss LA, Pople JA (1988) J Chem Phys 88:7405
25. Glukhovtsev MN, Bach RD (1998) Chem Phys Lett 286:51
26. Raine GP, Schaefer HF (1984) J Chem Phys 81:4034
27. DeFrees DJ, McLean AD (1985) J Chem Phys 82:333
28. Nefedova VV, Boldyrev AI, Simons J (1993) J Chem Phys 98:8801
29. Escribano R, Bunker PR (1987) J Mol Spectrosc 122:325
30. Escribano R, Bunker PR, Gomez PC (1988) Chem Phys Lett 150:60
31. Hougen JT (1987) J Mol Spectrosc 123:197
32. Tse JS, Klug DD, Laasonen K (1995) Phys Rev Lett 74:876
33. Marx D, Parrinello M (1996) Science 271:179

34. Knoll L, Vager Z, Marx D (2003) Phys Rev A 67:22506
35. Frisch MJ, Trucks GW, Schlegel HB, Scuseria GE, Robb MA, Cheeseman JR, Montgomery JA, Vreven T, Kudin KN, Burant JC, Millam JM, Iyengar S, Tomasi J, Barone V, Mennucci B, Cossi M, Scalmani G, Rega N, Petersson GA, Nakatsuji H, Hada M, Ehara M, Toyota K, Fukuda R, Hasegawa J, Ishida M, Nakajima T, Honda Y, Kitao O, Nakai H, Klene M, Li X, Knox JE, Hratchian HP, Cross JB, Bakken V, Adamo C, Jaramillo J, Gomperts R, Stratmann RE, Yazyev O, Austin AJ, Cammi R, Pomelli C, Ochterski J, Ayala PY, Morokuma K, Voth GA, Salvador P, Dannenberg JJ, Zakrzewski VG, Dapprich S, Daniels AD, Strain MC, Farkas Ö, Malick DK, Rabuck AD, Raghavachari K, Foresman JB, Ortiz JV, Cui Q, Baboul AG, Clifford S, Cioslowski J, Stefanov BB, Liu G, Liashenko A, Piskorz P, Komaromi I, Martin RL, Fox DJ, Keith T, Al-Laham MA, Peng CY, Nanayakkara A, Challacombe M, Gill PMW, Johnson B, Chen W, Wong MW, Pople JA (2004) Rev. C.02, Gaussian, Inc., Wallingford, CT
36. Krishnan R, Binkley JS, Seeger R, Pople JA (1980) J Chem Phys 72:650
37. Frisch MJ, Pople JA, Binkley JS (1984) J Chem Phys 80:3265
38. Raghavachari K, Trucks GW, Pople JA, Head-Gordon M (1989) Chem Phys Lett 157:479
39. Handy NC, Pople JA, Head-Gordon M, Raghavachari K, Trucks GW (1989) Chem Phys Lett 164:185
40. Dunning TH (1989) J Chem Phys 90:1007
41. Curtiss LA, Raghavachari K, Trucks GW, Pople JA (1991) J Chem Phys 94:7221
42. Curtiss LA, Raghavachari K, Redfern PC, Rassolov V, Pople JA (1998) J Chem Phys 109:7764
43. Ochterski JW, Petersson GA, Montgomery JA (1996) J Chem Phys 104:2598
44. Becke AD (1988) Phys Rev A 38:3098
45. Lee C, Yang W, Parr RD (1988) Phys Rev B 37:785
46. Becke AD (1993) J Chem Phys 98:5648
47. Burke K, Perdew JP, Wang Y (1988) In: Dobson JF, Vignale G, Das MP (eds) Electronic density functional theory: recent progress and new directions. Plenum Press, New York
48. Perdew JP, Burke K, Ernzerhof M (1996) Phys Rev Lett 77:3865
49. Tao JM, Perdew JP, Staroverov VN, Scuseria GE (2003) Phys Rev Lett 91:146401
50. Hratchian HP, Schlegel HB (2004) J Chem Phys 120:9918
51. Woodcock HL, Schaefer HF, Schreiner PR (2002) J Phys Chem A 106:11923
52. Schreiner PR, Fokin AA, Pascal RA, de Meijere A (2006) Org Lett 8:3635
53. Malick DK, Petersson GA, Montgomery JA (1998) J Chem Phys 108:5704